Rapid Process Parameter Discovery with Design of Experiments for Direct Ink Write Additive Manufacturing of Dense Pastes

Introduction:

"Printability" is a common metric of interest referred to in additive manufacturing (AM) literature [1-10], especially when dealing with bespoke printers and formulations. "Printability", however, has no formal definition -- it varies by configuration and need. When working to make new formulations for direct ink write (DIW) AM, it is especially difficult to formulate useful materials to print with when the target is unknown. Additionally, when dealing with complex materials like dense pastes, defined as suspensions with >50vol% solids [11], the problem is further complicated by time-dependent and memory-effect properties of the material at hand.

In hobbyist additive manufacturing, like SLA or FFF, there are benchmark artifacts used to calibrate a printer when using a known material like PLA or ABS. The much beloved Benchy [12] comes to mind, which when printed is qualitatively evaluated as by the user according to their experience and skill level. Other items, such as calibration cubes [13], can be printed and quantitatively evaluated with a caliper to check printer quality. In industry, there are more complicated and thoughtfully designed benchmark artifacts, such as for metal SLS processes [14], that enable tuning of a printer's settings or highlight a need for maintenance. These rely upon a well-qualified material that is known to be printable using specific print process parameters.

For direct ink write (DIW) AM of dense pastes, also referred to as 'inks', there currently exists no benchmark artifact, no definition of printability, and no way to isolate user and printer variation from the material to quantify material printability. Without first establishing a procedure for determining the print parameters used for the characterization of printability any measurement will be reliant on the user's experience and skill. By introducing a standardized method of rapidly determining print process parameters, the ideal print parameters for a material can be determined according to an adaptable value structure that meets an evolving definition of printability.

In this report, a process for determining a material's ideal print parameters using Design of Experiments (DOE) is described. By using DOE to vary print process parameters we can decouple the user's skill and experience from the measurement of a material's printability, enabling a more accurate assessment. Three print parameters factors were studied through line printing: print head speed, volumetric flow rate, and layer height. Five responses, measured via profilometry, were used to characterize the desirability of the resultant printed lines: area under the curve, variance in area under the curve, height variance, actual to set height ratio, and height to width ratio. 20 lines were printed with different combinations of settings and scanned to measure the response data. This enables the determination of statistically significant relationships between the factors and responses, resulting in the ability to predict response variables and overall line desirability from any given set of factors.

Materials, methods, and assumptions

Materials:

Paste:

All data reported here is using a formulation of bimodal melamine [15], at 78vol%, with a 3:1 coarse to fine ratio, that was mixed into a custom methacrylate binder system with a neat Newtonian viscosity of 0.35 Pa-s. Filler particle size distribution is shown below in figure 1.

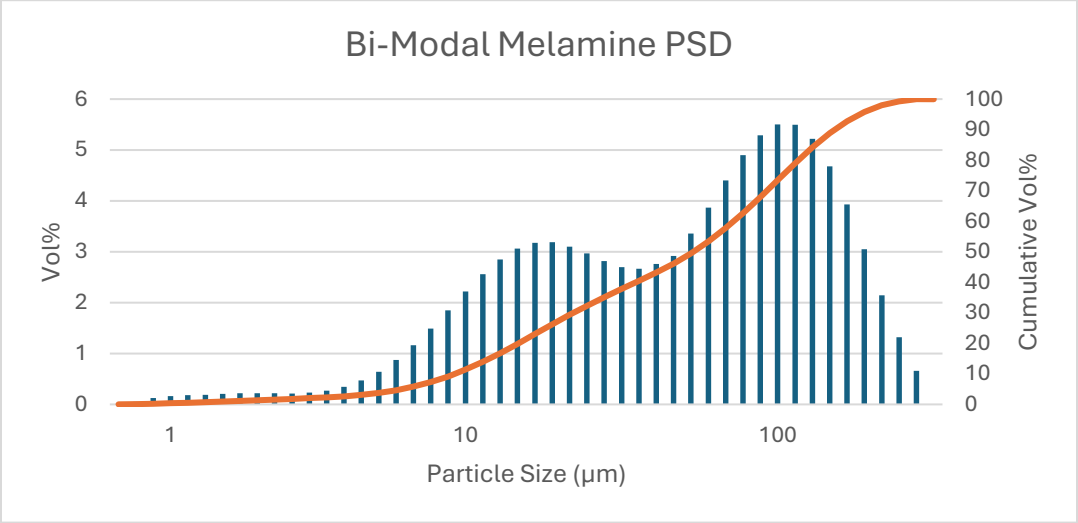

Figure 1: Melamine Particle Size Distribution

Paste density was calculated at 1.44 g/mL. The paste has a linear storage modulus (G'_{LVR}) of 2E+06 Pa [16] and a viscosity flow curve as shown below in figure 2 [17], with a consistency (K) of 3536 Pa-s^{n-1} and a Newtonian index (n) of 0.543

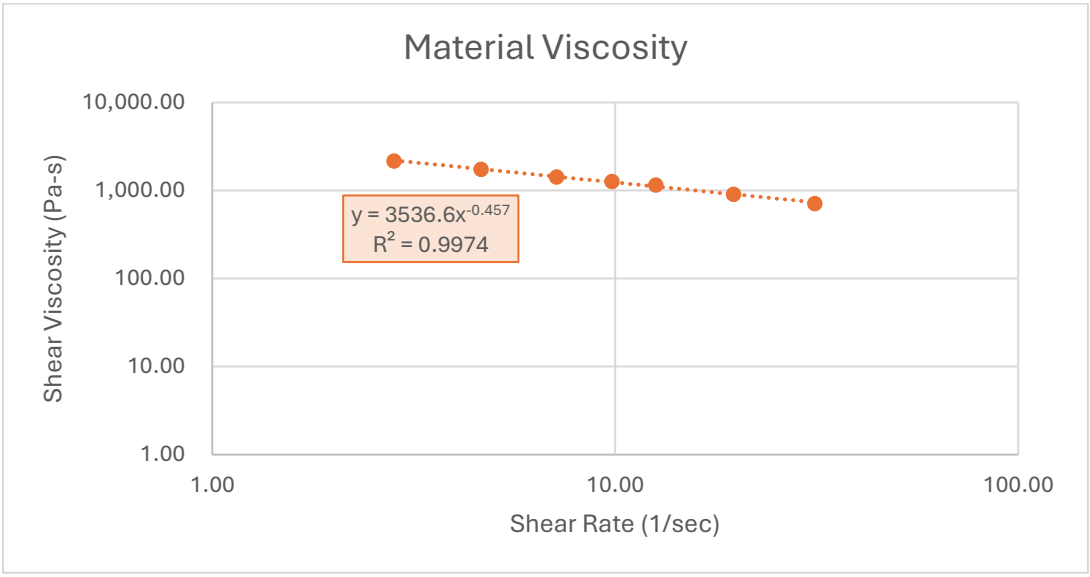

Figure 2: Formulation Viscosity

Mixer:

A FlackTek SpeedMixer 1200-300 VAC [18] was used to mix all of the inks in this paper. Mixing was done in accordance with the following procedure. All material for this report was mixed in one 100g batch, done in a 185mL container with a rounded bottom. After completing mixing the material was allowed to cool to room temperature, which took about 1 hour. Once at room temperature 15g of material was loaded into clear 10mL Nordson EFD syringes [19] which were centrifuged using a Cole-Parmer 17250-10 Fixed-Speed Centrifuge [20] to remove entrained air. These syringes were allowed to rest overnight before being used for printing.

Printer:

A Taz Lulzbot 6 [21] modified with a Viscotec Eco-Pen 330 [22] progressive cavity pump (PCP) was used for all printing in this report. The PCP was controlled via an Eco-Controller EC200 [23], also from Viscotec, that was commanded via a Python script communicating over RS-232 interfaces. Nordson ESD 10mL syringes with beige wipers were used to pneumatically fill the PCP with material. Air was supplied locally from a pressurized air cylinder. All materials were printed using a 16-gauge Luer-Lock tip from Nordson EFD that was 25.4mm long and had an ID of 1.54mm [24].

Profilometer:

Keyence VR-3000 [25] series profilometer was used to perform all 3D scans discussed in this report. The low magnification camera, at 12x, was used in all scans. Auto-focusing was used in all scans. All scans used anti-glare scanning mode and scanned both sides of printed items to achieve the highest accuracy of scan. When analyzing scan data, the print bed was used as the reference plane to establish a zero-height.

Software:

Python 3.11.5 [26] was used via the Spyder IDE Version 5 [27] to process data, produce summary statistics and visualizations in this report. The following Python packages used were: PySerial [28], pandas [29], matplotlib [30], SciPy [31], and NumPy [32]. JMP Pro 16 [33] was used to generate DoE designs and evaluate resultant data. Keyence software that is proprietary to the profilometer was used to generate some visualizations and export data.

Bespoke Hardware:

Two FFF additively manufactured arms were used as an interface for mounting the print bed onto the profilometer to enable the scanning of printed items without requiring removal from the print bed.

Methods:

Experiment Design

A custom DOE was designed to vary three print process parameter factors and evaluate how they impact the quality of a printed line as measured by five responses. The three input parameters evaluated were layer height, volumetric flow rate, and print speed.

The layer height varied between 0.64 and 0.92mm. These values were selected using the heuristic that layer height should be between 30-60% nozzle diameter and an integer multiple of

the z-step height, which for the printer in use is 0.04mm as determined by the z-screw geometry. Values below 0.5mm were regarded as too low and thus 0.64mm was arbitrarily selected as a lower bound that should be able to produce solid printable lines.

The volumetric flow rate for the PCP in use may vary between 0.2 and 3 mL/min. However, in using the PCP with dense paste materials it is not feasible to achieve these higher flow rates. Additionally, it is not functionally desirable to print at the lowest flow rates either, as the print time would be exceedingly long. Thus, bounds of 0.5-1.5 mL/min were selected as reasonable settings for the printer.

Print speed can very widely for the printer in use. However, as with volumetric flow rate, the materials in use constrain the feasible maximum print speeds. Additionally, there is a lower bound where printing is too slow, and some applicability is compromised. Thus, print speed bounds were set at 100-300 mm/min.

These factors are all related geometrically to each other via the width of the printed line, which is not controlled. At the same print speed and layer height a higher volumetric flow rate will produce a wider line. Similarly, at the same volumetric flow rate and layer height a faster print speed will produce a narrower line. By purposefully varying these parameters via a DOE we can accurately determine quantitative relationships between these factors, their interactions, and our responses of interest.

The DOE described herein investigated 5 such responses of interest. Each of these responses was given a target and a relative importance. The proximity to each of the target values, and the relative importance of the responses, determined the desirability of a combination of settings used in the DOE. Each response variable was measured using profilometry and the data post processed with Python.

The first response was the average percentage area under the curve (A-AUC %) for each line cross-section. The % area under the curve is defined as the ratio between the area of the line cross-section, the yellow in figure 3 below, and the rectangle it is inscribed within, the yellow and green. Thus, as this value approaches 1 the cross-section of the line becomes flatter on the top, less rounded on the sides, and more rectangular. The area under the curve is found in this way at multiple cross sections along the line and average to attain the A-AUC.

The target for this response was 1 – or 100% -- meaning that the ideal bead shape is rectangular in cross-section and is this way across many cross-sections of the line. This is, of course, not possible when using soft materials and a cylindrical nozzle. However, it serves to prioritize attaining a flat top for each bead and the overall consistency of the line cross-sectional area. This response was given the highest relative importance, 5.

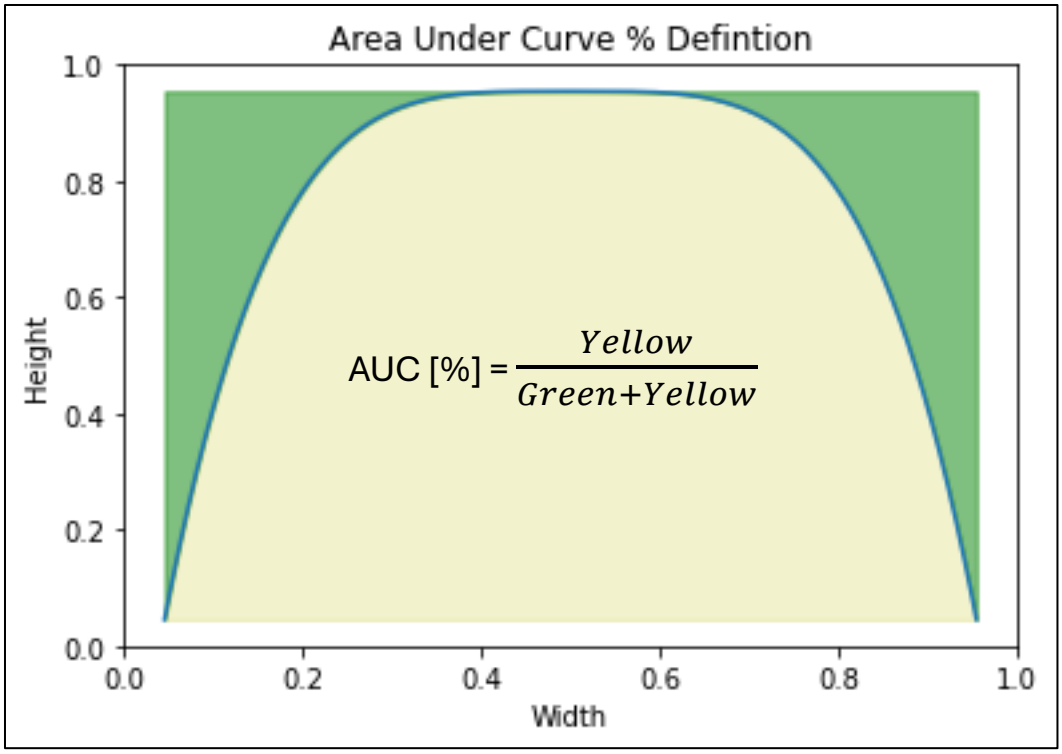

Figure 3: Definition of Area Under Curve %

The second response was the variance of the area under the curve (V-AUC %). This was found in the same way as response 1, only look at variance rather than average. This response was given a target of zero, no variance, or perfect consistency in bead cross section across the length of the bed. This response was given a relative importance of 2.

The third response was the variance in the height of the line. The target for this response was zero, corresponding with the goal of a consistent height across the length of the bed. This response was given a relative importance of 2. The fourth response was the average of the ratio of actual to set height. The target for this response is 1 – it is desired that the height assigned in the slicing software and g-code can be attained by the ink in use. Thus, this response was given a relative importance of 3. The fifth and final response was the average width to height ratio of the line. The target for this response was 3 – an arbitrarily selected value. The relative importance for this response was 1.

With these factors and responses, the DOE was additionally set up to include interactions between the factors, 4 center points and 4 replicate runs. No blocking or aliasing was used. This design required 20 runs, which was able to fit onto the print bed and in the scanning window of the profilometer. For this design the prediction power for each factor and interaction was 0.958 indicating a very good design that will enable strong conclusions upon its completion [34].

Design Execution:

After completing the design, a table was generated with 20 runs, each with a set value for layer height, print speed, and volumetric flow rate, as shown below in table 1.

Run	Layer Height	Volumetric Flow Rate [mL/min]	Print Speed [mm/min]
1	0.64	1.5	300
2	0.64	0.5	100
3	0.64	1.5	300
4	0.92	1.5	100
5	0.92	1.5	300
6	0.92	0.5	100
7	0.92	0.5	100
8	0.78	1	200
9	0.92	1.5	100
10	0.78	1	200
11	0.92	1.5	300
12	0.78	1	200
13	0.64	1.5	100
14	0.78	1	200
15	0.64	0.5	300
16	0.64	1.5	100
17	0.64	0.5	300
18	0.92	0.5	300
19	0.64	0.5	100
20	0.92	0.5	300

Table 1: DOE Run Definition

Before starting printing the printer was homed, the bed levelled, and the PCP purged. The printing of each line started at the bottom of the print plate (X = 50, Y = 50) and proceeded to the top (Y=250), in the y-direction. After each line was completed, extrusion was stopped, the print head moved a short distance in the x-axis, back to the starting point on the y-axis, and then the process was repeated. In this way each line was completed, from 1-20.

Profilometry:

After the lines were printed, they were allowed to rest for 30min before being analyzed on the profilometer. The entire tempered glass print bed was removed from the printer and mounted onto the profilometer. This enabled the scanning of printed items without disturbing them from their as-printed state. After the scan was complete the user selected horizontal profiles to obtain cross-sectional area data on all the printed lines.

Data Processing:

The output from the profilometer contains unit ID and height data, corresponding to the heights measured on the bed across the horizontal profile scanned. The unit ID refers to the horizontal position at which the height data point was taken. This unit ID can be converted to width by using the XY Calibration distance, 23.576 micron. Thus, each horizontal profile, taken at different

y positions, can be resolved into x and z data. At this point, each profile contains data for all the printed lines. It is required to break this larger dataset down into subsets for each line.

To do this, the data for each profile is imported into Python and refactored into datasets containing only x and z data for each DOE run. This can be done with many different profiles along the print bed and enables the measurement of x and z data for all lines across the entire print bed. With this data all responses can be measured and output from the Python script.

Assumptions:

The most critical assumption in this methodology is that the tempered glass print bed is flat. Additionally, it is assumed that any minor variations in the print bed are accounted for by the auto-levelling function performed before printing. It is also assumed that the positioning on the x-axis of the printed beads in the DOE does not determine their quality. Lastly, it is assumed that although the materials do exhibit time-dependent and memory-effect behaviors these characteristics are not operating on the timescale of the palette printing.

Results and Discussion

During the execution of the DOE to determine ideal print process parameters it was found that 4 of the runs were not able to produce lines. These were runs 15, 17, 18, and 20. Each of which operated at low volumetric flow rate (0.5 mL/min) and high print speed (300 mm/min). Thus, only 16 successful lines were written onto the print bed and scanned via profilometry. Additionally, the first line, shown on the leftmost side of the scan 3D model shown below in figure 4, had difficult adhering to the bed but was eventually able to establish a consistent line as it neared the middle/top of the scan window. Thus, all horizontal scan sections of the lines were taken in this region at the upper region section of the print bed.

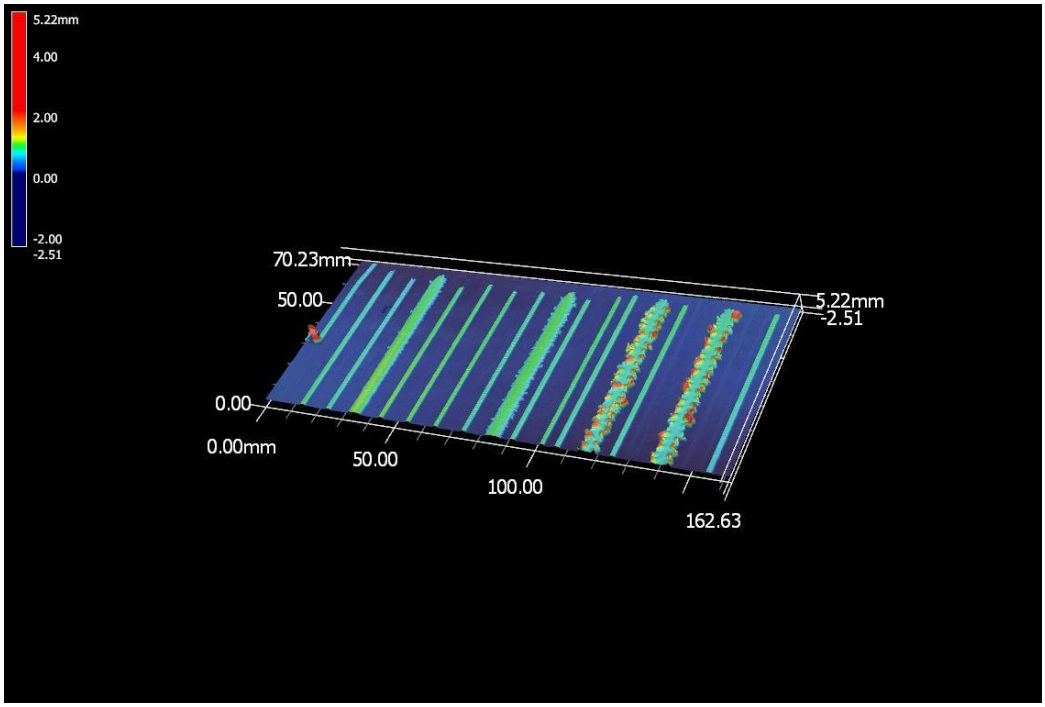

Figure 4: Scanned Lines 3D Image

As shown in the top left, red indicates taller structures while blue is the print bed that serves as the reference plane. From this scan it is shown that some settings produce narrow lines, others produce very wide lines, and yet others produce very jagged lines. There is no clear indication that the line behavior varies from left to right or top to bottom.

The scanned data was then broken down into 10 profiles to obtain horizontal cross-section data as shown below in figure 5.

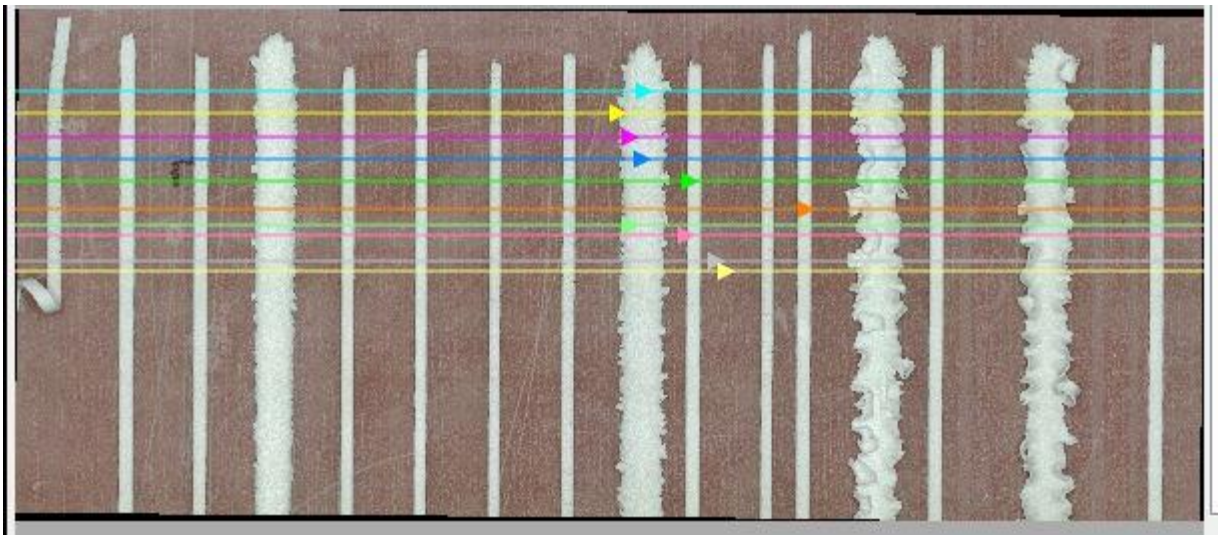

Figure 5: Profile Y-Position Definition

Each of the colored horizontal lines shown corresponds to a profile dataset that was created, containing x (width) and z (height) data for all beads, as shown in figure 6. Figure 6 is not to scale.

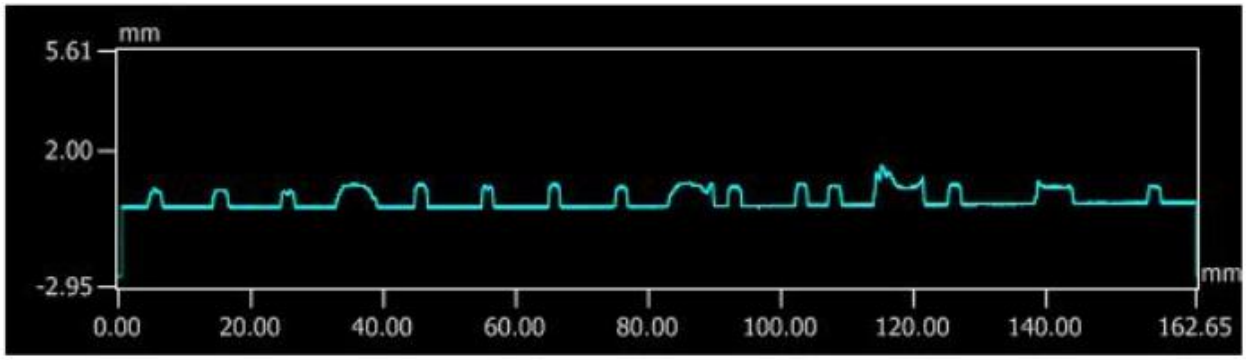

Figure 6: Full Profile Cross-Section Example

There were 10 total horizontal profiles taken at different y positions. Each of these were broken down to the subsets corresponding to each of the 16 lines, an example of which is shown in figure 7 below.

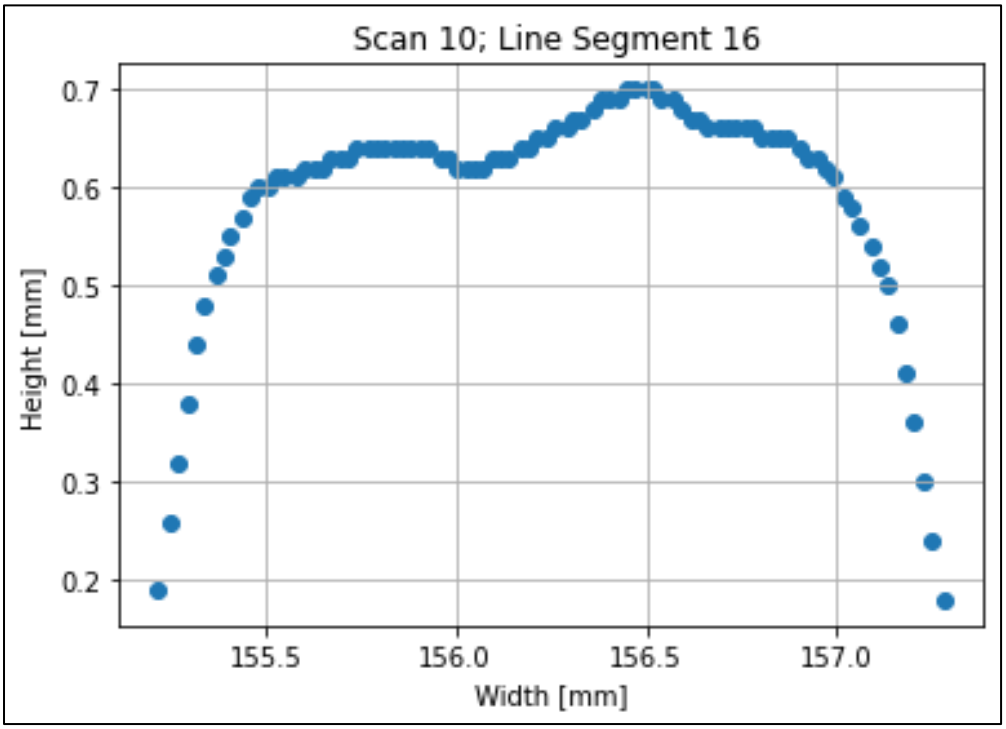

Figure 7: Profile Subset Example

The subsets were then recombined to produce complete datasets for each of the lines, each containing 10 sections of x-z at different y-positions along the bed. Table 1 below details the values obtained for the response variables.

Run	Factors			Responses				
	Layer Height [mm]	Volumetric Flow Rate [mL/min]	Print Speed [mm/min]	Area Under Curve [%], Average	Area Under Curve [%], Variance	Height [mm], Variance	Actual/Set Height, Average	Width/Height, Average
1	0.64	1.5	300	87%	0.002	0.001	1.01	3.18
2	0.64	0.5	100	89%	-	0.002	1.00	3.42
3	0.64	1.5	300	88%	-	0.002	0.95	3.34
4	0.92	1.5	100	81%	0.001	0.001	0.91	6.62
5	0.92	1.5	300	88%	-	0.001	0.90	2.29
6	0.92	0.5	100	88%	-	0.001	0.89	2.15
7	0.92	0.5	100	86%	-	-	0.90	2.07
8	0.78	1	200	86%	0.001	0.001	0.92	2.58
9	0.92	1.5	100	82%	-	-	0.90	7.45
10	0.78	1	200	88%	-	-	0.92	2.83
11	0.92	1.5	300	88%	-	-	0.89	2.20
12	0.78	1	200	89%	-	-	0.94	2.80
13	0.64	1.5	100	63%	0.011	0.188	2.36	4.48
14	0.78	1	200	87%	-	0.001	0.95	2.63
15	0.64	0.5	300	0%	-	-	-	-
16	0.64	1.5	100	48%	0.036	0.749	3.16	3.13
17	0.64	0.5	300	0%	-	-	-	-
18	0.92	0.5	300	0%	-	-	-	-
19	0.64	0.5	100	87%	-	0.001	1.07	3.02
20	0.92	0.5	300	0%	-	-	-	-

Table 2: DOE Results

For both V-AUC and height variance most of the readings were zero, or effectively zero. For the number of data points available, 10, and the differences detected variance is likely not the best measure of line consistency across the print bed. However, for the DOE runs where line print quality was very bad, namely runs 13 and 16, variance did quantify the lack of quality and penalize the

desirability of those settings. The low A-AUC numbers for these runs likely compensate enough for this low desirability and thus, in future DOE design, variance should be excluded.

From this data the DOE a least squares fit analysis can be done, which provides insight into how each response varied against the input factors. There is a detailed report for each response provided in the appendix. From the model effect summary, as shown below in table 3, it can be determined that each factor and each second order interaction is statistically significant in the prediction of the material's printability as defined by the responses detailed.

Effect Summary

Source	LogWorth	PValue
volumetric flow rate*print speed	5.390	0.00000
volumetric flow rate(0.5,1.5)	4.885	0.00001
print speed(100,300)	4.870	0.00001
layer height(0.64,0.92)	2.629	0.00235
layer height*print speed	2.376	0.00421
layer height*volumetric flow rate	2.205	0.00624

Table 3: DOE Effects Summary

Based on this effect summary, we can say that the most important factor is the interaction between print speed and volumetric flow rate. This makes physical sense: as we increase our print speed, we must increase our volumetric flow rate to maintain a solid line. Otherwise, we may over or under-extrude. As we read down this list we can see the priority order of each factor.

The goal of this work was to determine the ideal print process parameters as measured by the responses defined in this DOE. For this purpose, the prediction profiler is the best tool to observe the desirability of different combinations of print parameters. The overall prediction profiler is shown below in figure 8.

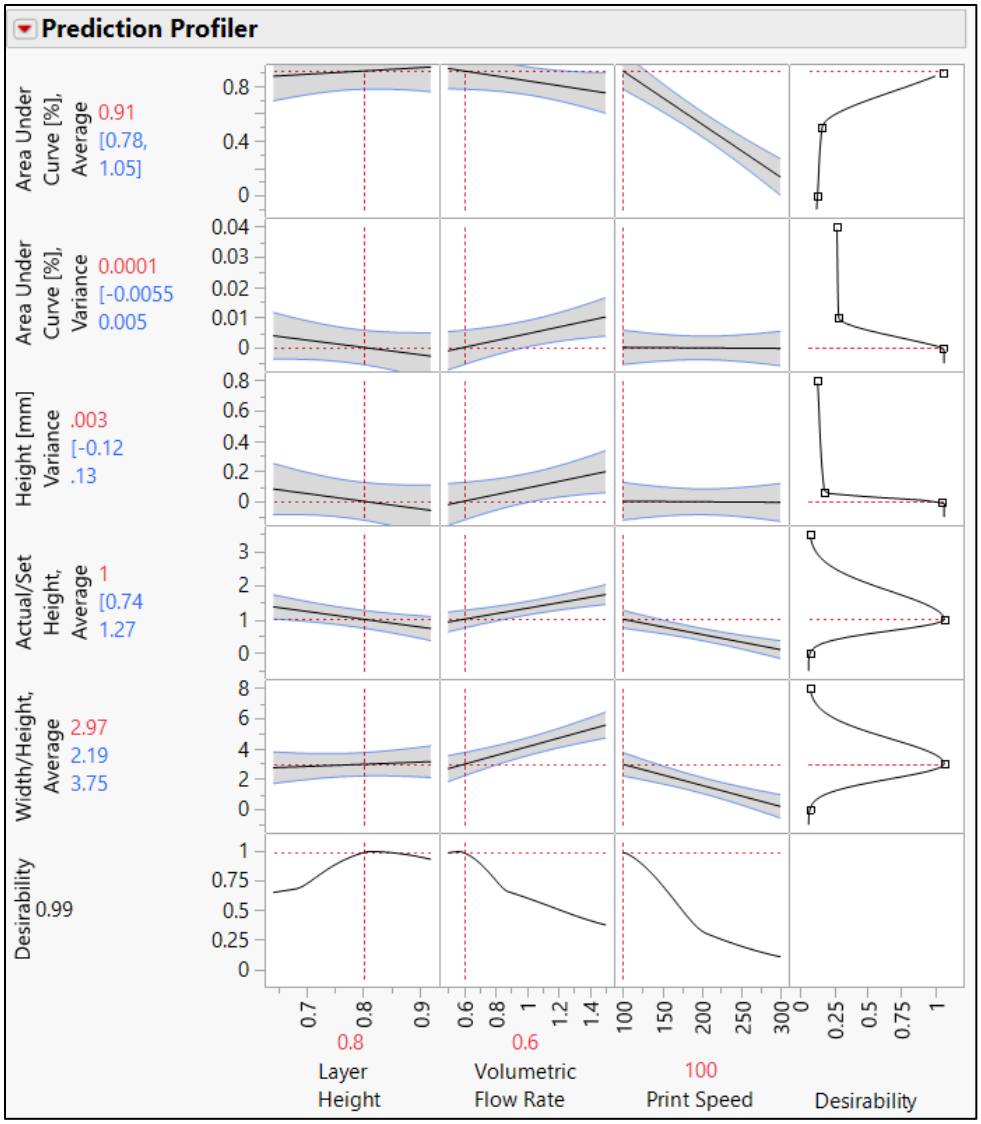

Figure 8: DOE Prediction Profiler

On the right-hand side, we can see the definitions of desirability for each response: maximizing A-AUC, minimizing V-AUC, minimizing height variance, and targeting specific values for set/actual height and width/height ratio – 1 and 3 respectively. Based off these definitions, the ideal print parameters can be found. These ideal print parameters are shown at the bottom, namely: layer height of 0.8mm, volumetric flow rate of 0.6 mL/min, and a print speed of 100 mm/min. This should result in a A-AUC of 91%, a V-AUC and height variance of effectively zero, an actual/set height ratio of 1, and a width/height ratio of 2.97. From these values the expected width can also be calculated, as 2.38mm.

Here the versatility of this process is highlighted. By printing 20 lines, a process that takes less than an afternoon once the inks are ready, the experimenter can elucidate the trade space of their print parameters. From there, they can change how they define value within each of these responses or take a single response of interest and predict its value based off the analysis available. The responses can be varied as required. However, for distributed analysis the

community must agree upon a quantitative definition of a what enables 2D and 3D construction most successfully and codify this into a DOE procedure like the one described here.

Conclusions

"Printability" is a widely desired, but difficult to measure or define parameter for any material. This challenge is further amplified when working with dense pastes. To properly define "printability" for dense pastes in DIW the experimenter must contend with three major sources of variation: the user, printer, and material. When seeking to characterize the usefulness of a material in printing it is critical to eliminate the sources of variation from the user and printer as much as possible. The methodology proposed in this report leverages a DOE framework, consisting of a limited number of simple test prints, scanned via profilometry, that can identify the ideal print process parameters for a new formulation, thus eliminating user variation caused by arbitrary print process parameter selection. This methodology was demonstrated through the printing of 20 straight lines and the production of a statistically significant least square model fit. This model was used to predict the most desirable print parameters as defined by five responses: average area under the curve, variance in area under the curve, height variance, the actual to set height ratio, and the height to width ratio. For 78vol% formulation of melamine, with a 3:1 coarse to fine ratio, in a thin binder system, printed with a PCP, these ideal print process parameters were a volumetric flow rate of 0.6 mL/min, layer height of 0.8mm, and print speed of 100mm/min.

Using this DOE process these parameters can be statistically determined in a rapid, yet flexible, manner. This allows for the quick determination of parameters that can be used to print a benchmark artifact that will further eliminate the printer's variation and focus in solely on the material's printability. Further, once determined, the definition of desirability used to select the parameters can be adjusted to meet developing needs for an ink as use cases change. This work in determining the ideal print process parameters via DOE paves the way towards the development of a benchmark artifact for DIW AM of dense pastes that will be the tool for defining and quantifying material printability in a standard way; and, thus enabling the rapid, distributed evaluation of formulations for DIW AM.

Path ahead:

This work demonstrates only a small portion of a larger set of ideas that can be pursued in this space. Follow on work to this may go in many directions, but there are a few that the author can anticipate currently. The incorporation of bed meshing techniques, using a BL-touch, or the like, would greatly eliminate many of the assumptions in this report. Further, including the x-position, and run #, in the DOE would help eliminate any concerns about bed positioning and/or behavioral changes of the material throughout the DOE.

There are additional methods that could be conducted before or after this process to enhance the overall process of evaluating a materials "printability". Before moving to print a DIW DOE, the experimenter could verify their gantry performance and bed-level by printing a benchmark artifact via FFF on the same printer. This would help eliminate any concerns that the perceived characterization of the material may be a characterization of the printer. Additionally, a DIW

benchmarking process could be done with a simpler material, such as DOWSIL SE17000, before moving into this process with a dense paste. This would help isolate any variations seen to the material and ensure that the printer in use works as desired.

The next report in this series will cover the development of a benchmark artifact for DIW AM of dense pastes. That report will take the print parameters determined here and apply them to the construction of basic shapes and structures. These will be scanned, again with profilometry, and their overall dimensional fidelity interpreted as their printability. After determining the print parameters as discussed here the width is calculated, and this will be assumed to be the ideal center to center distance between the lines in a printed item. However, this will introduce voids [35] into the material and for this reason there is value in expanding this DOE directly, or doing another one subsequently, to observe how varying the center-to-center distance between the lines impacts their ability to coalescence into one layer.

After statistically determining the ideal print process parameters, by maximizing response desirability, a benchmark artifact can be developed that will enable the measurement of printability using those parameters. The development of a benchmark artifact to define and quantify printability will be covered in a subsequent report.

References:

[1] Daniel A. Rau, Christopher B. Williams, Michael J. Bortner, Rheology and printability: A survey of critical relationships for direct ink write materials design, Progress in Materials Science, Volume 140, 2023, 101188, ISSN 0079-6425, https://doi.org/10.1016/j.pmatsci.2023.101188

[2] Peiran Wei, Ciera Cipriani, Chia-Min Hsieh, Krutarth Kamani, Simon Rogers, Emily Pentzer; Go with the flow: Rheological requirements for direct ink write printability. *J. Appl. Phys.* 14 September 2023; 134 (10): 100701. https://doi.org/10.1063/5.0155896

[3] Dimpy Bhardwaj, Ritu Singhmar, Megha Garg, Deepika Gupta, Ankita Dhiman, Sung Soo Han, Garima Agrawal, Designing advanced hydrogel inks with direct ink writing based 3D printability for engineered biostructures, European Polymer Journal, Volume 205, 2024, 112736, ISSN 0014-3057, https://doi.org/10.1016/j.eurpolymj.2023.112736

[4] M'Barki, A., Bocquet, L. & Stevenson, A. Linking Rheology and Printability for Dense and Strong Ceramics by Direct Ink Writing. *Sci Rep* **7**, 6017 (2017). https://doi.org/10.1038/s41598-017-06115-0

[5] Aleksei Dolganov, Matthew T. Bishop, George Z. Chen, Di Hu, Rheological study and printability investigation of titania inks for Direct Ink Writing process, Ceramics International, Volume 47, Issue 9, 2021, Pages 12020-12027, ISSN 0272-8842, https://doi.org/10.1016/j.ceramint.2021.01.045

[6] Qingyang Zheng et al 2023 Int. J. Extrem. Manuf. 5 035002

[7] *Polymers* 2022, *14*(21), 4661; https://doi.org/10.3390/polym14214661

[8] M. A. S. R. Saadi, A. Maguire, N. T. Pottackal, M. S. H. Thakur, M. Md.Ikram, A. J. Hart, P. M. Ajayan, M. M. Rahman, Direct Ink Writing: A 3D Printing Technology for Diverse Materials. *Adv. Mater.* 2022, 34, 2108855. https://doi.org/10.1002/adma.202108855

[9] Chan SSL, Sesso ML, Franks GV. Direct ink writing of hierarchical porous alumina-stabilized emulsions: Rheology and printability. *J Am Ceram Soc*. 2020; 103: 5554–5566. https://doi.org/10.1111/jace.17305

[10] Myoeum Kim, Jae-Won Choi, Rubber ink formulations with high solid content for direct-ink write process, Additive Manufacturing, Volume 44, 2021, 102023, ISSN 2214-8604, https://doi.org/10.1016/j.addma.2021.102023

[11] Marnot, A., Dobbs, A. & Brettmann, B. Material extrusion additive manufacturing of dense pastes consisting of macroscopic particles. *MRS Communications* **12**, 483–494 (2022). https://doi.org/10.1557/s43579-022-00209-1

[12] #3DBenchy - The jolly 3D printing torture-test by CreativeTools.se by CreativeTools – Thingiverse: https://www.thingiverse.com/thing:763622

[13] XYZ 20mm Calibration Cube by iDig3Dprinting – Thingiverse : https://www.thingiverse.com/thing:1278865

[14] S.P. Moylan, J.A. Slotwinski, A.L. Cooke, K.K. Jurrens, and M.A. Donmez (2012), "Proposal for a standardized test artifact for additive manufacturing machines and processes," Proceedings of the 23rd International Solid Free Form Symposium – An Additive Manufacturing Conference, Austin, TX, USA, August 2012, pp. 902-920.

[15] Melamine SDS: https://documentation.oci-global.com/wp-content/uploads/2023/01/OCI-Nitrogen-MelaminebyOCI-Safety-Data-Sheet-GPH-GPH-LD-SLP-Melafine-IE.pdf

[16] Author's own ongoing research, forthcoming report

[17] Author's own ongoing research, forthcoming report

[18] Medium FlackTek™ - The FlackTek™: https://flacktek.com/products/medium-flacktek/

[19] Optimum® Syringe Barrels | Nordson EFD: https://www.nordson.com/en/products/efd-products/optimum-syringe-barrels

[20] Centrifuge Spec: https://cms.esi.info/Media/documents/ColeP_centrifuges_ML.pdf

[21] LulzBot | Taz-6: https://assets.lulzbot.com/TAZ6_SpecSheet_FINAL.pdf

[22] eco-PEN330: https://epotekeurope.com/wp-content/uploads/2022/08/preeflow-datenblatt-eco-pen-englisch-2020.pdf

[23] EN eco CONTROL EC200 2.0: https://dosieren.de/media/29/9a/6e/1708524623/EN_eco_CONTROL_EC200_2.0_Betriebs-und-Wartungsanleitung_Version-2023.pdf

[24] Dispense Tips and Needles | Optimum® Dispense Tips | Nordson EFD: https://nc-p-001.sitecorecontenthub.cloud/api/public/content/763d342ed9b24b6380265648d916dab1?v=99ca5481

[25] 3D Optical Profilometer - VR-6000 series | KEYENCE America: https://www.keyence.com/products/3d-measure/roughness-measure/vr-6000/

[26] Python Release Python 3.11.5 | Python.org: https://www.python.org/downloads/release/python-3115/

[27] Install Guide — Spyder 5 documentation: https://docs.spyder-ide.org/5/index.html

[28] pyserial · PyPI: https://pypi.org/project/pyserial/

[29] pandas · PyPI: https://pypi.org/project/pandas/

[30] matplotlib · PyPI: https://pypi.org/project/matplotlib/

[31] scipy · PyPI: https://pypi.org/project/scipy/

[32] numpy · PyPI: https://pypi.org/project/numpy/

[33] Predictive Analytics Software | JMP Pro: https://www.jmp.com/en_is/software/predictive-analytics-software.html

[34] Power Analysis: https://www.jmp.com/support/help/14/power-analysis.shtml

[35] Sungwoo Jang, Andrew Boddorff, Dong June Jang, Jacob Lloyd, Karla Wagner, Naresh Thadhani, Blair Brettmann, Effect of material extrusion process parameters on filament geometry and inter-filament voids in as-fabricated high solids loaded polymer composites, Additive Manufacturing, Volume 47, 2021, 102313, ISSN 2214-8604, https://doi.org/10.1016/j.addma.2021.102313.